

## EFFECT OF SURFACTANTS (CETYL TRIMETHYL AMMONIUM-BROMIDE, ETHYL DI-TETRA AMINE AND POLYACRYLAMIDE) ON THE SYNTHESIS OF ZINC OXIDE FOR PHOTOCATALYTIC APPLICATION

Hulugirgesh Degefu Weldekirstos\*, Muluken Zerie, Daniel Manaye, Abebe Tedla\* and Asfaw Negash

Department of Chemistry, Debre Brehan University, Debre Brehan, Ethiopia

(Received December 30, 2023; Revised March 28, 2024; Accepted April 1, 2024)

**ABSTRACT.** In this work, we report the effect of cetyl trimethyl ammonium bromide (CTAB), ethyl di-tetra amine (EDTA) and polyacrylamide as surfactants on synthesis of zinc oxide for photocatalytic application. The ZnO nanoparticles were synthesized with and without the surfactants and characterized using powder X-ray diffraction (PXRD), and Fourier transform infrared spectroscopy (FTIR). In addition to this, the morphology of zinc oxide prepared in the absence and presence of these surfactants investigated through scanning electron microscopy (SEM). As confirmed from XRD and FTIR characterization results, the use of different surfactants did not affect the composition of ZnO nanomaterials. The photocatalytic activities were investigated by the degradation of methylene blue (MB) dye under sunlight irradiation. To optimize the effects of operational parameters, the study was carried out as a function of dye concentration, catalyst dose, and pH on the degradation efficiency of the photocatalysts. The optimum values of catalyst dose, dye concentration and pH of solution were found to be 0.09 g, 5 mg/L and 10, respectively. The ZnO nanomaterials prepared with CTAB surfactant showed highest degradation efficiency of 98% indicating potential application for practical decontamination of wastewater from toxic organic pollutants.

**KEY WORDS:** Surfactants, Zinc oxide nanoparticles, Photocatalysis, Methylene blue

### INTRODUCTION

Environmental contamination, which is growing around the world, is a serious problem not to be neglected. Among all contamination, water pollution is a major problem [1]. One of the most pressing environmental issues of the present and most probably of the future is the effective protection and utilization of the precious freshwater resources of the world. 88% of the 4 billion annual cases of diarrheal disease are attributed to unsafe water and inadequate sanitation and hygiene, and 1.8 million people die from diarrheal diseases each year, all over the world [2]. The World Health Organization (WHO) estimates that 94% of these diarrheal cases are preventable through modifications to the environment, including access to safe water. Estimations of today's water situation are frightening. Just to mention some numbers: 1.1 billion people are without clean drinking water and about 4000 children die every day from water borne diseases [3]. In Ethiopia's context also as research reports indicated that getting quality water is becoming challenge with the expansion of different industries and wastes which caused to water pollution [4, 5].

The dyeing process does not utilize all the dye molecules and consequently a substantial number of dyes were present in the wastewater released from the industry [6-8]. The photocatalysis process towards eliminating an organic pollutant from water or air has numerous potential applications to resolve serious environmental pollution [9-12]. In a photocatalytic system, photo-induced molecular transformation or reaction takes place at the surface of the catalyst. A basic mechanism of photocatalytic reaction on the generation of electron-hole pair and its destination is as follows. When a photocatalyst is illuminated by the light stronger than its

---

\*Corresponding authors. E-mail: HulugirgeshDegefu@dbu.edu.et, huludeg21@gmail.com, (Hulugirgesh D.W.); abebetedla@gmail.com (Abebe Tedla)

This work is licensed under the Creative Commons Attribution 4.0 International License

band gap energy, electron migrates from valance band (VB) to conduction band (CB) and holes are formed in valance band. These holes can generate hydroxyl radicals which are highly oxidizing in nature. Probably hole can react with dye molecule and abstract electron from dye molecule and process of degradation proceed [13, 14].

Transition metal oxides have attracted tremendous attention from researchers owing to their easy synthesis and ability to form various phases of metal–oxygen ratios possessing different structure, properties, and applications. Metal oxide semiconductors such as zinc oxide, titanium dioxide, tungsten oxide, and zinc stannite applied for photocatalysis and important during water purification and removal of organic pollutants [15]. Zinc oxide (ZnO) is a type II-VI semiconductor with a direct band gap of 3.37 eV and stable wurtzite type structure with lattice parameters  $a = 3.25 \text{ \AA}$  and  $c = 5.21 \text{ \AA}$  [2, 16-22]. It is an important semiconductor material due to its applications, which include transparent conductive oxides (TCO) [23], ultraviolet (UV) blockers, and photo catalysts, among others. Zinc oxide nanoparticles have nontoxic nature, wide band gap, and good quantum efficiency [24, 25].

The electron mobility of ZnO ( $\sim 100 \text{ cm}^2 \text{ V}^{-1} \text{ s}$ ) is approximately two orders of magnitude higher than TiO<sub>2</sub> based nanomaterials. Thus, it is easier for the photogenerated charge carriers to migrate towards the surface of ZnO based nanomaterials. ZnO has also been proven to be useful in the removal of toxic metal ions as well as harmful microorganisms such as *Escheria coli* and *Staphylococcus aureus* [26]. Surfactants are well known in surface modification during material synthesis [27].

The main concern of this work is to investigate the influence of surfactants type on the synthesis of zinc oxide for photocatalytic application. In order to investigate the influence of surfactants on the preparation and photocatalytic activity of ZnO, EDTA as nonionic, CTAB as cationic and polyacrylamide were used. The molecular structure of these surfactants are shown in Figure 1.

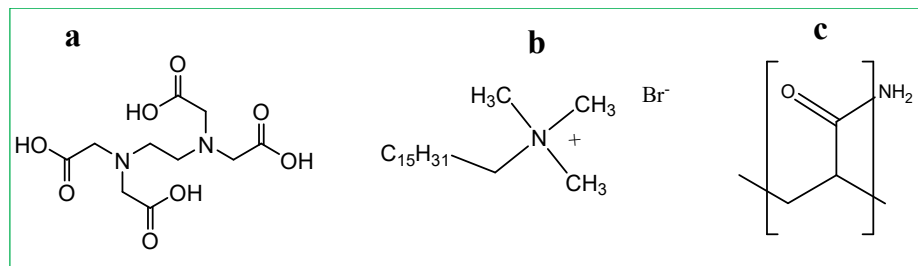


Figure 1. Chemical structures of EDTA (a), CTAB (b) and polyacrylamide (c).

## EXPERIMENTAL

### Chemicals

The chemicals and reagents used for this study were hydrochloric acid (HCl) 37%, sodium hydroxide (NaOH) pellets (98%), Alphax Chemical Industry (India), NaCl (0.1N), methylene blue (MB) SAMHR TECH-CHEM PVT-LTD, zinc chloride (ZnCl<sub>2</sub>), sodium hydroxide (NaOH), deionized water, HCl, and CTAB, EDTA, and polyacrylamide. All chemicals used in this study were of analytical grade.

*Synthesis of ZnO with and without surfactants*

The synthesis of ZnO nanoparticle is based on the solvothermal method. An amount of 4.2 g (0.01 mol) of  $\text{ZnCl}_2$  and 1 g of CTAB, 1 g of EDTA, 1 g of polyacrylamide was dissolved in 100 mL of distilled water in three different 250 mL Schott bottle and stir for 30 minutes, then heated to a temperature of 60 °C with constant stirring using electrical stirring hotplate. Subsequently, 4.1 g (0.01 mol) of NaOH was also weighed and dissolved in 100 mL of in 250 mL Schott bottle under the same condition as the Zinc precursor. The NaOH solution was slowly drained drop wise from a burette into the  $\text{ZnCl}_2$  solution, maintaining the temperature at 60 °C with vigorous stirring for 60 min until a white precipitate was formed. The mixture cooled at room temperature for 180 min before centrifuging with FLETA 5 Multi-Purpose Centrifuge at 4000 rpm for 30 min. The precipitate was washed at least 5 times with deionized water, dried at room temperature, and finally ground into a powdered form and calcinated at 450 °C for 3 h [28]. The general procedure presented in Figure 2.

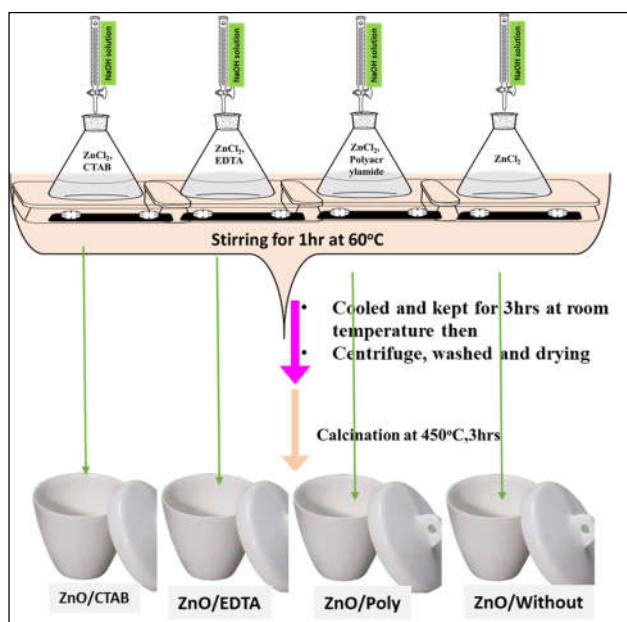


Figure 2. Synthesis route for ZnO nanoparticles using CTAB, EDTA, polyacrylamide surfactants and without surfactant.

*Photocatalytic activity study*

The photocatalytic studies were performed to investigate the performance of ZnO nanomaterials synthesized using different surfactants for the degradation MB under sun light irradiation. 0.1 g of the photocatalyst was added into 100 mL of 10 mg/L solution of MB. Before photocatalysis, the solution was stirred magnetically for 60 min in the dark to establish an adsorption-desorption equilibrium. At a fixed time, interval 3 mL of suspension was collected for recording the absorbance at  $\lambda_{\text{max}} = 664 \text{ nm}$  a maximum MB. The pH of the solutions was adjusted by adding either 0.1 M HCl or 0.1 M NaOH. The degradation (%) efficiency was computed using Eq. 1. The

photocatalytic performance of ZnO, ZnO/CTAB, ZnO/EDTA and ZnO/poly were investigated at various contact time, initial concentrations of MB (5, 10, 15, 20, 30 mg/L), pH of solution (2, 4, 6, 8, 10) and dose of photo-catalyst (25 mg to 150 mg).

$$\text{Degradation (\%)} = \left( \frac{C_0 - C_t}{C_0} \right) \times 100 \quad (1)$$

where  $C_0$  is initial concentration of MB dye and  $C_t$  is the concentration of MB dye at time  $t$ .

#### Characterization techniques

Powder X-ray diffraction (PXRD) used to determine the phase structure of the samples such as the crystallinity of the catalyst and measure their size. Fourier transform infrared spectroscopy (FTIR) is implemented to identify the presence of certain functional groups in a given sample. Scanning electron microscopy (SEM) applied to interpret the morphology difference. UV-Visible absorption spectroscopy also used to investigate photocatalytic degradation efficiency MB dye.

## RESULTS AND DISCUSSION

#### FTIR analysis

Figure 3 presents the FTIR spectra of asynthesized samples in the presence of EDTA, CTAB and polyacrylamide. The band observed between 421 and 559  $\text{cm}^{-1}$  in all samples corresponds to Zn–O stretching mode which confirms the formation of ZnO. In addition to this, the weak peak at 890  $\text{cm}^{-1}$  indicates the presence of –OH bending peaks [29, 30].

Almost all FTIR peaks of the synthesized samples ZnO, ZnO with EDTA, and ZnO with CTAB were the same as clearly indicated in Figure 3. For ZnO-WO, ZnO-CTAB and ZnO-EDTA, the weak peaks presented between 1300  $\text{cm}^{-1}$  and 1610  $\text{cm}^{-1}$  could be C=O and C–H vibration bands probably from trace residue to the coatings [31]. These weak peaks of C=O and C–H vibration bands didn't appear on ZnO-polyacrylamide sample and this observation is consistent with the previous findings [32].

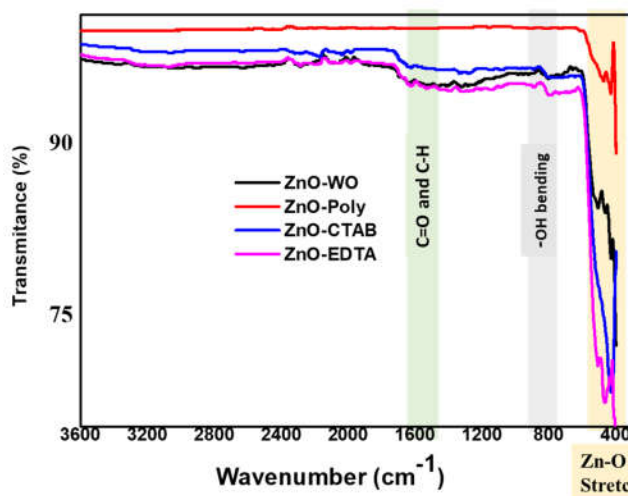


Figure 3. FTIR spectra of ZnO nanoparticles synthesized using CTAB, EDTA and polyacrylamide.

### PXRD analysis

The powder X-ray diffraction (PXRD) patterns of as prepared materials (zinc oxide without surfactants, zinc oxide with cetyl trimethyl ammonium bromide, zinc oxide with ethyl di-tetra amine and zinc oxide with polyacrylamide hereafter named as ZnO-WO, ZnO-CTAB, ZnO-EDTA and ZnO-polyacrylamide, respectively) are presented in Figure 4. In all the four materials, the well observed peaks appeared at  $2\theta = 31.9^\circ, 34.5^\circ, 36.3^\circ, 47.5^\circ, 56.5^\circ, 63^\circ, 66.5^\circ, 68^\circ, 69.1^\circ$  and  $77^\circ$  prove that ZnO is approaching the hexagonal structure. The characteristic diffraction peaks marked by their indices (100), (002), (101), (102), (110), (103), (200), (112), (201) and (202) respectively could be well indexed to the structure of ZnO. According to the X-ray diffraction patterns in Figure 4, the ZnO samples prepared in the presence of different surfactants revealed sharp and narrow peaks, indicating good crystallinity. The observed peaks confirmed to 100, 002, 101, 102, 110, 103, 200, 112, and 201 Miller indices, which correspond to a hexagonal quartzite structure of ZnO (ICSD card no. 57450), similar to those reported by Muhammad *et.al.* [33]. The average crystallite size of the samples was determined using the Debye-Scherer formula as indicated in Eq. 2:

$$D = \frac{k\lambda}{\beta \cos\theta} = \frac{0.9\lambda}{\beta \cos\theta} \quad (2)$$

where D is the average crystallite size in nm, k is a shape factor constant equal to 0.9,  $\lambda$  is the wavelength of the x-ray used (CuK $\alpha$  radiation = 1.5406 Å),  $\beta$  is the full width at half maximum. As the result, the calculated. The average crystal size of the samples was shown in the Table 1.

Table 1. Average crystallite size (D) of as-synthesized photo-catalysts.

Sample	$2\theta$ (degree)	D (nm)
ZnO-WO	36.254	46
ZnO-CTAB	36.218	20
ZnO-EDTA	36.251	43
ZnO-poly	36.219	28

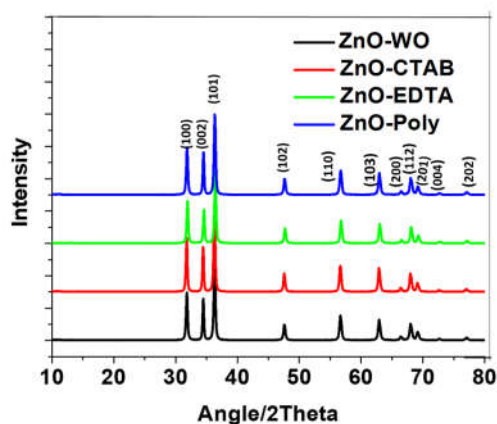


Figure 4. PXRD of ZnO nanoparticles prepared in the presence of different surfactants (CTAB, EDTA, and polyacrylamide).

### Morphology investigation

The morphological influence of using different surfactants during the preparation of nanomaterials have been carried out using scanning electron microscopic technique. SEM images of ZnO nanoparticles prepared in the presence of different surfactants (CTAB, EDTA, and Polyacrylamide) presented in Figure 5 (a-d). When ZnO was synthesized in the absence of surfactant, the obtained SEM image have aggregated and packed morphology as presented in Figure 5a. Whereas when ZnO synthesized in the presence of EDTA, the SEM image of the prepared sample have a nanosheet morphology (Figure 5b). When CTAB was used as surfactant during the preparation of ZnO, the morphology was changed to spherical nanoparticles as demonstrated in Figure 5c. On the other hand, when the surfactant used was polyacryl amide, the ZnO morphology looked like nanoleaves (Figure 5d). From the difference in SEM images, it could be explained that the surfactants used during the preparation of ZnO affected the morphological structure of ZnO nanoparticles.

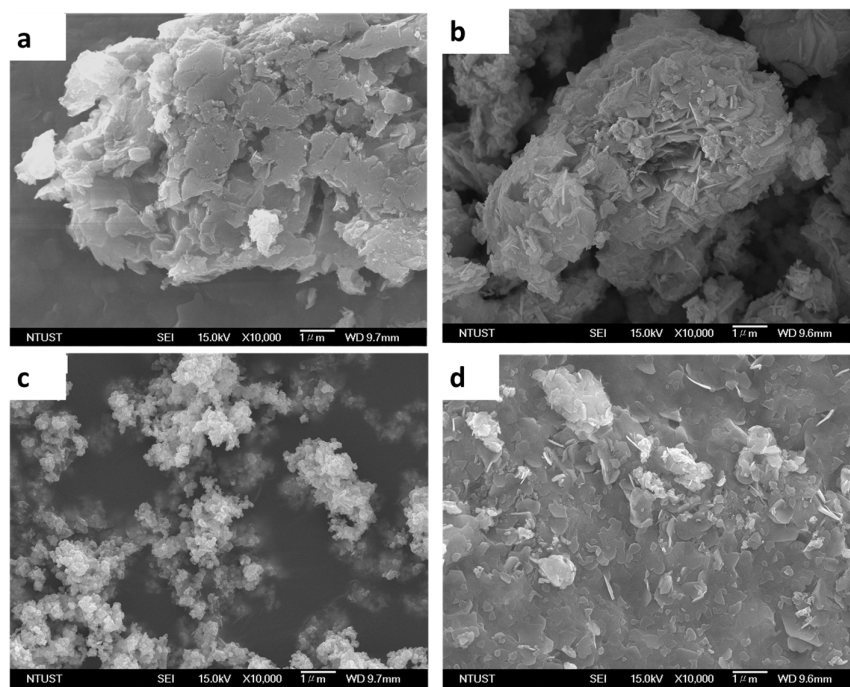


Figure 5. SEM images of ZnO nanoparticles prepared in the presence and absence of different surfactants: ZnO-WO (a), ZnO-EDTA (b), ZnO-CTAB (c) and ZnO-polyacrylamide (d)

### Point of zero charge

The degradation of organic dyes on the adsorbent surface was primarily affected by the surface charge on the adsorbent which in turn is influenced by the solution pH. The point of zero charge analysis was used to investigate the surface charge of photocatalyst surface as a function of pH. For the general principle, if the pH is higher than the point of zero charge, the surface of the photocatalyst will be charged negatively and therefore it repulses anion compounds and vice

versa. At  $\text{pH} < \text{pH}_{\text{PZC}}$ , the degrading surface may be positively charged due to protonation of the carboxyl and other functional groups [34]. The point of zero charges of ZnO-WO, ZnO-CTAB, ZnO-EDTA and ZnO-polyacrylamide were presented in Figure 6. From the findings shown in Figure 6, the point of zero charge values for ZnO, ZnO prepared using CTAB, EDTA and polyacrylamide were obtained as 6.7, 7.3, 6.7, and 7.1, respectively. Therefore, at higher pH ( $\text{pH} \geq 7.3$ ), the adsorbent surface has a negative charge and decolorize the cationic methylene blue dye via electrostatic attraction.

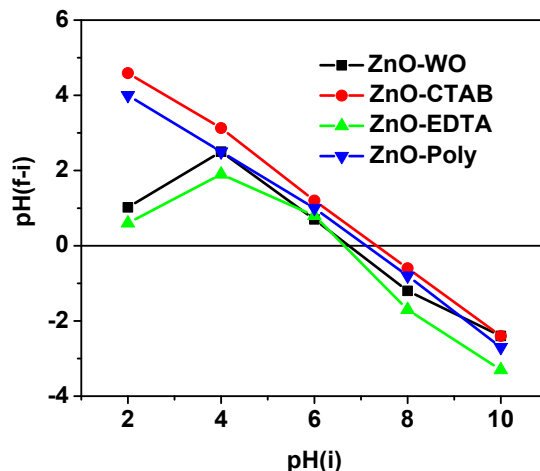


Figure 6. Point of zero charge of ZnO-WO, ZnO-CTAB, ZnO-EDTA and ZnO-polyacrylamide.

#### Photocatalytic parameters optimization

**Effect of pH.** The influence of pH on the degradation of MB in the presence of ZnO-WO, ZnO-CTAB, ZnO-EDTA and ZnO-polyacrylamide was investigated at initial pH value varying between 2 to 10 and the results presented in Figure 7A. As shown in Figure 7A, the percentage degradation of MB using all newly synthesized photocatalysts was enhanced with a rise in solution pH up to 8. At smaller acidic pH, a lower removal was observed due to the competitive interactions of  $\text{H}^+$  and cationic MB. Upon increasing pH from 8.0 to 10.0, the MB degradation showed slightly decreases. After the dye removal was completed, the pH value of 8 with the highest degradation efficiency was taken as the optimum pH. From the four photocatalysts, ZnO-CTAB achieved highest efficiency throughout the measurement.

**Effect of dye concentration.** The dependence of the degradation efficiency of ZnO-WO, ZnO-CTAB, ZnO-EDTA and ZnO-polyacrylamide at various initial concentrations of MB dye (5, 10, 15, 20 and 25 mg/L) presented in Figure 7B. The percentage of degradation in the presence of these synthesized photocatalysts increased with decrease in initial dye concentrations throughout the measurement as revealed in Figure 7B. Generally, at low concentrations of organic pollutants, the rate of degradation increases with the increase of substrate concentration since there are sufficient amounts of radicals and holes for the reaction with contaminants at low substrate concentration. However, beyond the optimal concentration, the removal rate decreases due to the insufficient number of reactive radicals [35].

*Effect of photocatalyst amount.* The effect of amounts of ZnO-WO, ZnO-EDTA, ZnO-CTAB and ZnO-polyacrylamide towards photocatalytic degradation of MB were investigated at 0.01, 0.03, 0.05, 0.07 and 0.09 g as the results shown in Figure 7C. The measurements were carried out at a fixed concentration of MB (10 mg/L). It was found that by increasing the adsorbent dose, the percentage of dye removal also increases. It implies that the number of available degradation sites increases by increasing the adsorbent dose and resulted in an increase in the percentage of dye removal. As shown in Figure 7C, the ZnO-CTAB material achieved the highest degradation efficiency of 68.5%, 74.5%, 76.7%, 97.8%, 98.1% at 0.01, 0.03, 0.05, 0.07 and 0.09 g, respectively.

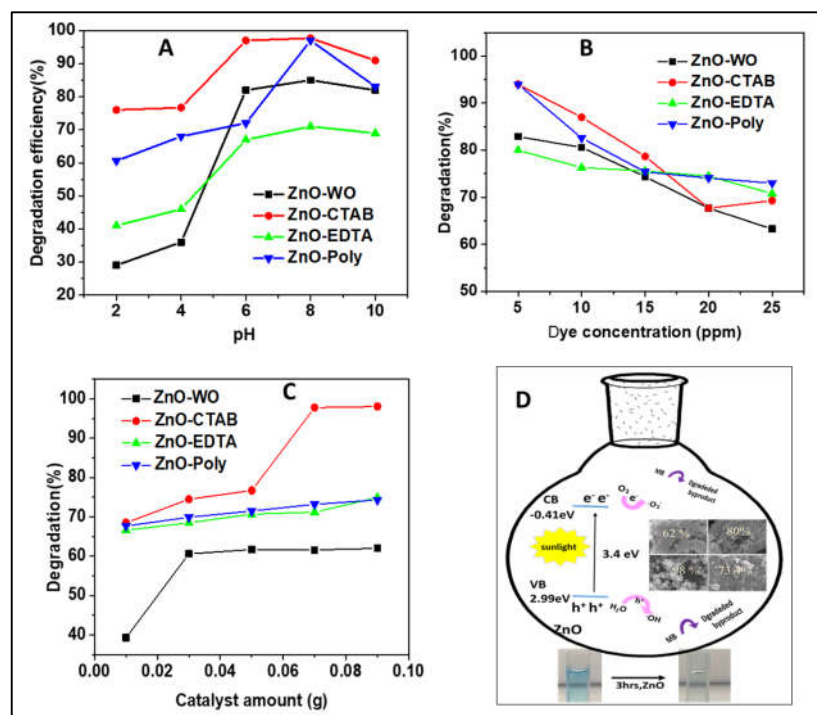


Figure 7. A) Effect of pH, B) effect of MB dye concentration and C) effect of photocatalyst dose on the photocatalytic degradation efficiency of the synthesized photocatalysts towards MB dye, D) the proposed mechanism of photocatalytic degradation of MB dye on the ZnO/CTAB nanoparticle.

#### Photocatalytic mechanism

The proposed schematic mechanism of photocatalytic degradation of methylene blue on the ZnO was shown in Figure 7 D. While the solution is exposed to visible light irradiation, the electrons would be excited from the VB to the CB. The photo-generated electrons would further reduce the dissolved oxygen to produce superoxide radicals, which would oxidize MB to final degraded products of carbon dioxide and water. On the other side the photo-generated holes at the VB of reacted with water from the solution and produced hydroxide radicals can subsequently oxidize



the MB to generate CO<sub>2</sub> and H<sub>2</sub>O [36]. To explain the photocatalytic mechanism, the valence band (VB) and conduction band (CB) potentials of ZnO/CTAB was calculated using Eq. 3 and Eq.4:

$$E_{CB} = \chi - E_{ef} - 0.5 E_g \quad (3)$$

$$E_{VB} = E_{CB} + E_g \quad (4)$$

where  $E_{CB}$  is the CB edge potential;  $E_{VB}$  is the VB edge potential;  $\chi$  is the semiconductor electronegativity;  $E_{ef}$  is the energy of free electrons on the hydrogen scale (about 4.5 eV) [37];  $E_g$  is the semiconductor band gap energy.  $\chi$  value of 5.79 eV [38].  $E_g$  is obtained as 3.4 eV for ZnO-CTAB calculated from UV-Vis absorption measurement using  $E_g = \frac{1240}{\lambda}$ . The VB and CB of ZnO-CTAB obtained as 2.99 eV and -0.41 eV, respectively.

#### Kinetics of the photocatalytic degradation

Recent studies on photocatalytic reactions have been performed using the pseudo-first-order kinetics with respect to the substrate concentration [39]. To ensure the reaction order, both pseudo-first- and pseudo-second-order kinetics were tested. The integrated forms of the pseudo-first- and pseudo-second-order models are according to Eq. 5 and Eq. 6, respectively.

$$\ln\left(\frac{C_0}{C_t}\right) = k_{obs1} t \quad (5)$$

$$\frac{1}{C} = \frac{1}{C_0} + k_{obs2} t \quad (6)$$

where  $C_0$ ,  $C_t$ ,  $k_{obs1}$  and  $k_{obs2}$  represent the initial concentrations of MB, the concentration of MB at time  $t$ , observed pseudo-first- and pseudo-second-order rate coefficients, respectively. The plots of  $\ln(C_0/C_t)$  and  $1/C$  versus  $t$  at different initial MB concentrations are plotted in Figure 8A and Figure 8B, respectively.

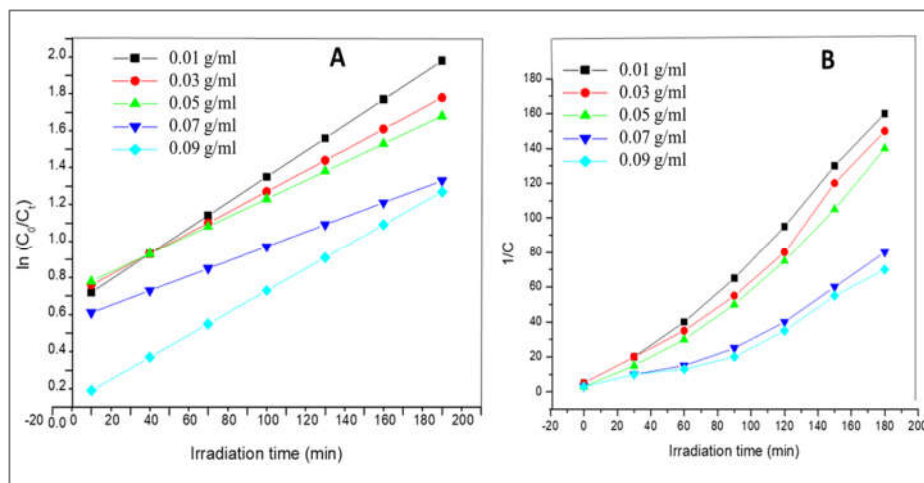


Figure 8. The plots of  $\ln(C_0/C_t)$  versus irradiation time (A) and the plots of  $1/C$  versus irradiation time (B) at different initial MB concentrations.

*Comparison with the previous reports*

The comparison of the obtained degradation efficiency of synthesized photo-catalysts with previously reported findings has been illustrated in Table 2. Our findings showed that ZnO synthesized using CTAB as surfactant attained the highest photo-degradation efficiency for methylene blue dye removal.

Table 2. Comparison of photocatalytic performance and synthesis strategy of zinc oxide toward the degradation of methylene blue dye.

Photo-catalyst	Synthesis method	Light source	Degradation efficiency (%)	References
Ni/NiO/ZnO	One-pot solution combustion synthesis	Ultraviolet Irradiation	15	[40]
N-doped ZnO	Co-precipitation	Visible light	93	[41]
2%Fe-ZnO	Sol-gel	150 W mercury light	92	[42]
ZnO-leaf extract	Co-precipitation	Sunlight	96.5	[43]
ZnO-CTAB	Co-precipitation	Sunlight	98.1	This work
ZnO-EDTA	Co-precipitation	Sunlight	80.0	This work
ZnO-Polyacrylamide	Co-precipitation	Sunlight	73.4	This work
ZnO-without	Co-precipitation	Sunlight	62	This work

**CONCLUSION**

In this study, we have reported the influence of EDTA, CTAB, and polyacrylamide surfactants on the synthesis of ZnO through ecofriendly co-precipitation method. The crystalline property of the synthesized materials was characterized through PXRD and the results confirmed as pure ZnO material was prepared. SEM also applied to understand the morphology difference resulted when different surfactants used for the synthesis of ZnO based materials. The surface charge properties of these synthesized materials also studied through the point of zero-charge analysis. The photocatalytic performance of the synthesized ZnO using different surfactants were tested for MB removal. The photocatalytic parameters: pH, photocatalyst amount and dye concentration has been optimized. The photocatalytic degradation efficiencies towards MB dye were achieved about 98.1% using ZnO-CTAB, 73.4% using ZnO-polyacrylamide, 80% using ZnO-EDTA, and 62% using ZnO without surfactant. The results indicated that the ZnO/CTAB exhibited excellent photocatalytic activity as compared to ZnO-polyacrylamide, ZnO-EDTA, and ZnO without surfactant toward the degradation of MB under sunlight irradiation.

**ACKNOWLEDGMENTS**

The authors would like to thank Department of Chemistry, Debre Brehan University for providing materials support.

**REFERENCES**

1. Kilic, Z. Water pollution: Causes, negative effects and prevention methods. *İstanbul Sabahattin Zaim Üniversitesi Fen Bilimleri Enstitüsü Dergisi* **2021**, 3, 129-132.
2. Mukherjee, D. Development of novel photo catalyst for water purification under solar and UV light. *PhD Thesis*, The University of Western Ontario London, Ontario, Canada, **2011**.

3. The United Nations World Water Development Programme Report 3: Water in a changing world, UNESCO, **2009**.
4. Lewoyehu, M. Evaluation of drinking water quality in rural area of Amhara region, Ethiopia: The case of Mecha district. *J. Chem.* **2021**, 2021, 1-11.
5. Daniel, T.D.; Fitamo, D.F.; Abate, B.A.; Osore, A.O. Assessment of the quality of drinking water supply, and the status of sanitation and hygiene in Mudulla Town, Tembaro Woreda, Southern Ethiopia. *Civil Environ. Res.* **2016**, 8, 67-78.
6. Katheresan, V.; Kannedo, J.; Lau, S.Y. Efficiency of various recent wastewater dye removal methods: A review. *J. Environ. Chem. Eng.* **2018**, 6, 4676-4697.
7. Bilal, M.; Rasheed, T.; Sosa-Hernández, J.E.; Raza, A.; Nabeel, F.; Iqbal, H. Biosorption: An interplay between marine algae and potentially toxic elements—a review. *Mar. Drugs* **2018**, 16, 65.
8. Anju, A.; Ravi, S.P.; Bechan, S. Water pollution with special reference to pesticide contamination in India. *Water Resour. Prot.* **2010**, 2, 432-448.
9. Ismael, M. Structure, properties, and characterization of mullite-type materials  $\text{Bi}_2\text{M}_4\text{O}_9$  and their applications in photocatalysis: a review. *J. Environ. Chem. Eng.* **2022**, 10, 108640.
10. Ismael, M. Environmental remediation and sustainable energy generation via photocatalytic technology using rare earth metals modified  $\text{g-C}_3\text{N}_4$ : A review. *J. Alloys Compd.* **2022**, 931, 167469.
11. Ismael, M. Latest progress on the key operating parameters affecting the photocatalytic activity of  $\text{TiO}_2$ -based photocatalysts for hydrogen fuel production: A comprehensive review. *Fuel* **2021**, 303, 121207.
12. Ismael, M. A review on graphitic carbon nitride ( $\text{g-C}_3\text{N}_4$ ) based nanocomposites: Synthesis, categories, and their application in photocatalysis. *J. Alloys Compd.* **2020**, 846, 156446.
13. Kislov, N.; Lahiri, J.; Verma, H.; Goswami, D.Y.; Stefanakos, E.; Batzill, M. Photocatalytic degradation of methyl orange over single crystalline ZnO: Orientation dependence of photoactivity and photostability of ZnO. *Langmuir* **2009**, 25, 3310-3315.
14. Yaser, A.Z.; Pogaku, R. Recent trends for the removal of colored particles in industrial wastewaters. *Environ. Sci. Pollut. Res.* **2017**, 24, 15861-15862.
15. Jurablu, S.; Farahmandjou, M.; Firoozabadi, T. Sol-gel synthesis of zinc oxide (ZnO) nanoparticles: study of structural and optical properties. *J. Sci. I. R. Iran* **2015**, 26, 281-285.
16. Nagaraja, R.; Kottam, N.; Girija, C.; Nagabhushana, B. Photocatalytic degradation of Rhodamine B dye under UV/solar light using ZnO nanopowder synthesized by solution combustion route. *Powder Technol.* **2012**, 215, 91-97.
17. Wouters, R.D.; Muraro, P.C.L.; Druzian, D.M.; Viana, A.R.; de Oliveira Pinto, E.; da Silva, J.K.L.; Vizzotto, B.S.; Ruiz, Y.P.M.; Galembeck, A.; Pavoski, G. Zinc oxide nanoparticles: Biosynthesis, characterization, biological activity and photocatalytic degradation for tartrazine yellow dye. *J. Mol. Liq.* **2023**, 371, 121090.
18. Murali, R.; Amirthavalli, C. Defect assisted reactive oxygen species generation for photocatalytic degradation of methylene blue by nano-structured zinc oxide synthesized in CTAB medium. *Mater. Chem. Phys.* **2023**, 294, 127014.
19. Huong, Le M.; Cong, C.Q.; Dat, N.M.; Hai, N.D.; Nam, N.T.H.; An, H.; Do Dat, T.; Dat, N.T.; Phong, M.T.; Hieu, N.H. Green synthesis of carbon-doped zinc oxide using *Garcinia mangostana* peel extract: Characterization, photocatalytic degradation, and hydrogen peroxide production. *J. Clean. Prod.* **2023**, 392, 136269.
20. Ifijen, I.H.; Maliki, M.; Anegebe, B. Synthesis, photocatalytic degradation and antibacterial properties of selenium or silver doped zinc oxide nanoparticles: A detailed review. *OpenNano.* **2022**, 8, 100082.
21. Dihom, H.R.; Al-Shaibani, M.M.; Mohamed, R.M.S.R.; Al-Gheethi, A.A.; Sharma, A.; Khamidun, M.H.B. Photocatalytic degradation of disperse azo dyes in textile wastewater

- using green zinc oxide nanoparticles synthesized in plant extract: A critical review. *J. Water Process Eng.* **2022**, *47*, 102705.
22. Bhattacharjee, N.; Som, I.; Saha, R.; Mondal, S. A critical review on novel eco-friendly green approach to synthesize zinc oxide nanoparticles for photocatalytic degradation of water pollutants. *J. Environ. Anal. Chem.* **2022**, *104*, 1-28.
  23. Ye, Z.; Li, J.; Zhou, M.; Wang, H.; Ma, Y.; Huo, P.; Yu, L.; Yan, Y., Well-dispersed nebula-like ZnO/CeO<sub>2</sub>@ HNTs heterostructure for efficient photocatalytic degradation of tetracycline. *Chem. Eng. J.* **2016**, *304*, 917-933.
  24. Chen, J.P. *Decontamination of Heavy Metals: Processes, Mechanisms, and Applications*; CRC Press: Florida; **2012**.
  25. Weldekirstos, H.D.; Habtewold, B.; Kabtamu, D.M. Surfactant-assisted synthesis of NiO-ZnO and NiO-CuO nanocomposites for enhanced photocatalytic degradation of methylene blue under UV light irradiation. *Fmats* **2022**, *9*, 832439.
  26. Kim, J.; Yong, K. A facile, coverage controlled deposition of Au nanoparticles on ZnO nanorods by sonochemical reaction for enhancement of photocatalytic activity. *J. Nanoparticle Res.* **2012**, *14*, 1-10.
  27. Weldekirstos, H.D.; Kuo, M.-C.; Li, S.-R.; Su, W.-L.; Desta, M.A.; Wu, W.-T.; Kuo, C.-H.; Sun, S.-S. New 2,3-diphenylquinoxaline containing organic DA- $\pi$ -A dyes with nickel oxide photocathode prepared by surfactant-mediated synthesis for high performance p-type dye-sensitized solar cells. *Dyes Pigm.* **2019**, *163*, 761-774.
  28. Shamhari, N.M.; Wee, B.S.; Chin, S.F.; Kok, K.Y. Synthesis and characterization of zinc oxide nanoparticles with small particle size distribution. *Acta Chim. Slov.* **2018**, *65*.
  29. Gnanasangeetha, D.; SaralaThambavani, D. One pot synthesis of zinc oxide nanoparticles via chemical and green method. *Res. J. Mater. Sci.* **2013**, *2320*, 6055.
  30. Siuleiman, S.; Raichev, D.; Bojinova, A.; Dimitrov, D.; Papazova, K. Nanosized composite ZnO/TiO<sub>2</sub> thin films for photocatalytic applications. *Bulg. Chem. Commun.* **2013**, *45*, 649-654.
  31. Rani, B.; Punniyakoti, S.; Sahu, N. K. Polyol asserted hydrothermal synthesis of SnO<sub>2</sub> nanoparticles for the fast adsorption and photocatalytic degradation of methylene blue cationic dye. *New J. Chem.* **2018**, *42*, 943-954.
  32. Halvaeifard, R.; Sharifnia, S. The effect of surfactants on the photocatalytic performance of BiOCl-ZnO nanoparticles in the degradation of an organic pollutant. *Korean J. Chem. Eng.* **2018**, *35*, 770-776.
  33. Adiwibowo, M.T.; Ibadurrohman, M.; Slamet, S. Synthesis of ZnO nanoparticles and their nanofluid stability in the presence of a palm oil-based primary alkyl sulfate surfactant for detergent application. *Int. J. Technol.* **2018**, *9*, 307-316.
  34. Elamin, N.; Elsanousi, A. Synthesis of ZnO nanostructures and their photocatalytic activity. *J AIS* **2013**, *1*, 32-35.
  35. Singh, J.; Chang, Y.-Y.; Koduru, J. R.; Yang, J.-K. Potential degradation of methylene blue (MB) by nano-metallic particles: A kinetic study and possible mechanism of MB degradation. *Environ. Eng. Res.* **2017**, *23*, 1-9.
  36. Duangjam, S.; Wetchakun, K.; Phanichphant, S.; Wetchakun, N. Hydrothermal synthesis of novel CoFe<sub>2</sub>O<sub>4</sub>/BiVO<sub>4</sub> nanocomposites with enhanced visible-light-driven photocatalytic activities. *Mater. Lett.* **2016**, *181*, 86-91.
  37. Ye, L.; Liu, J.; Gong, C.; Tian, L.; Peng, T.; Zan, L. Two different roles of metallic Ag on Ag/AgX/BiOX (X = Cl, Br) visible light photocatalysts: surface plasmon resonance and Z-scheme bridge. *ACS Catal.* **2012**, *2*, 1677-1683.
  38. Ye, Z.; Li, J.; Zhou, M.; Wang, H.; Ma, Y.; Huo, P.; Yu, L.; Yan, Y. Well-dispersed nebula-like ZnO/CeO<sub>2</sub>@ HNTs heterostructure for efficient photocatalytic degradation of tetracycline. *Chem. Eng. J.* **2016**, *304*, 917-933.

39. Senthilraja, A.; Subash, B.; Dhatshanamurthi, P.; Swaminathan, M.; Shanthi, M. Photocatalytic detoxification of Acid Red 18 by modified ZnO catalyst under sunlight irradiation. *Spectrochim. Acta Part A: Mol. Biomol. Spectrosc.* **2015**, 138, 31-37.
40. Biglari, Z.; Masoudpanah, S.; Alamolhoda, S. Solution combustion synthesis of Ni/NiO/ZnO nanocomposites for photodegradation of methylene blue under ultraviolet irradiation. *J. Electron. Mater.* **2018**, 47, 2703-2709.
41. Ramos-Corona, A.; Rangel, R.; Alvarado-Gil, J.; Bartolo-Pérez, P.; Quintana, P.; Rodríguez-Gattorno, G. Photocatalytic performance of nitrogen doped ZnO structures supported on graphene oxide for MB degradation. *Chemosphere* **2019**, 236, 124368.
42. Isai, K.A.; Shrivastava, V.S. Photocatalytic degradation of methylene blue using ZnO and 2% Fe-ZnO semiconductor nanomaterials synthesized by sol-gel method: a comparative study. *SN Appl. Sci.* **2019**, 1, 1-11.
43. Negash, A.; Mohammed, S.; Weldekirstos, H.D.; Ambaye, A.D.; Gashu, M. Enhanced photocatalytic degradation of methylene blue dye using eco-friendly synthesized rGO@ZnO nanocomposites. *Sci. Rep.* **2023**, 13, 22234.